Progress Towards a Validated Cantera-based Turbulent Flame Speed Solver

Eoin M. Burke [*,1], Alessandro Singlitico [1], Anibal Morones [2], Eric L. Petersen [2], Felix Güthe [3], BiruteBunkute[3], Raymond L. Speth [4], Rory F.D. Monaghan [1]

[1] Mechanical Engineering and Combustion Chemistry Centre, National University of Ireland, Galway, Ireland
[2]Department of Mechanical Engineering,Texas A&M University, College Station, TX 77843, USA
[3]Alstom, 5401 Baden, Switzerland
[4]Laboratory for Aviation and the Environment, Massachusetts Institute of Technology, 77 Massachusetts Ave., Cambridge, MA 02139, USA

Abstract
The aim of this work is to develop a Cantera-based solver to predict turbulent flame speeds (S_T) in the wrinkled flamelet, corrugated flamelet and thin reaction zone regimes, in which $Da > 1$. The existing unstretched, freely-propagating, one-dimensional laminar flame speed solver within Cantera was modified to include (1) enhancement of property transport, (2) enhancement of effective reaction rate, and (3) reduction of available reaction volume. With the modified solver S_T hydrogen/air mixtures over the range of equivalence ratios $0.5 \leq \Phi \leq 1.0$, at initial temperature and pressure of T_i = 300 K and P_i = 1 atm were calculated. Comparison with experimentally-obtained values and a currently-used correlation for S_T shows satisfactory agreement. Future work includes solver numerical improvements and validation for hydrocarbon fuels at different levels of turbulence.

Introduction

Combustion of fuels in gas turbines accounts for over 20% [1] of global electricity generation. Increasingly stringent emissions rules mean that gas turbine manufacturers must be able to certify low-emissions operation over a range of compositions and load levels. The ability to investigate operating conditions for low emissions is enabled by numerical modelling using detailed chemical kinetic mechanisms. Most industrially-applicable combustion occurs at turbulent conditions, the ability for researchers to validate their mechanisms at comparable conditions is highly desirable. Available one-dimensional (1D) flame speed solvers focus on laminar flames[2-3], These solvers are not capable of predicting turbulent flame speed (S_T) as they do not account for (1) enhanced transport, (2) reduction of available reaction volume, and (3) enhancement of effective reaction rate that are found in turbulent flow when compared to laminar.

The aim of this work is to develop a Cantera-based S_T solver which will account for the properties listed above. Enhancement of property transport due to turbulent mixing is modelled using a one-dimensional k-ε approach. Enhancement of effective reaction rate due to temporal temperature fluctuations is modelled using reaction rate correction factors that assume temperature distribution around a temporal mean. Reduction of available reaction volume due to the presence of fine turbulent structures is modelled using the eddy dissipation concept (EDC)[4].

In this paper, an overview of the progress made in developing the turbulent solver is described. An outline for the laminar solver and details of the modifications to enable turbulent predictions are discussed. The modified solver is tested against measurements of S_T for hydrogen/air mixtures over the range of equivalence ratios $0.5 \leq \Phi \leq 1.0$, at an initial temperature and pressure of T_i = 300 K and P_i = 1 atm, respectively. The effect of each new turbulent property is reviewed. Current limitations and future work are also discussed.

Method

The S_T solver is built on top of the existing unstretched freely-propagating, one-dimensional laminar flame speed (S_L) solver within Cantera 2.2a[5]. When calculating S_L, Cantera computes steady-state solutions to the mass, species and energy conservation equations, (1) to (3), for a reactive gaseous mixture. The conservation equations [6] are expressed as:

$$\frac{d\dot{m}''}{dx} = 0 \qquad \textbf{(1)}$$

$$\nabla \cdot (\rho u Y_i) = \nabla \cdot J_i + R_i \quad \text{where } J_i = -\rho D_i \nabla Y \qquad \textbf{(2)}$$

$$\nabla \cdot (u(\rho E + P)) = \nabla \cdot \left(\lambda \nabla T - \sum_i h_i \overline{J_i} \right) + S \qquad \textbf{(3)}$$

In these equations, x denotes the distance from the burner; $\dot{m}''$ is mass flux; ρ is density; u is velocity of the mixture; Y_i is

[*]Corresponding Authour: e.burke18@nuigalway.ie

mass fraction of species *i*; J_i is diffusive flux of species *i*; R_i is the source term for species *i*; D_i is diffusion coefficient of species *i* in the mixture; *E* is internal energy; *P* is pressure; λ is thermal conductivity; *T* is temperature; h_i is specific enthalpy of species *i; S* is net heat production due to reactions.

As Cantera is a relatively new modelling tool, its performance for the prediction of S_L using GRI3.0 [7] for hydrogen-air premixtures over the range of equivalence ratios $0.5 \leq \Phi \leq 2.5$, at initial temperature and pressure of T_i = 300 K and P_i = 1 atm is compared to the widely-used CHEMKIN PRO solver [2] and experimental data [8]. The results of this comparison are shown in Figure 1 and show close similarity in solutions. To account for the effects of turbulence on flame speed, Cantera needed to be modified.

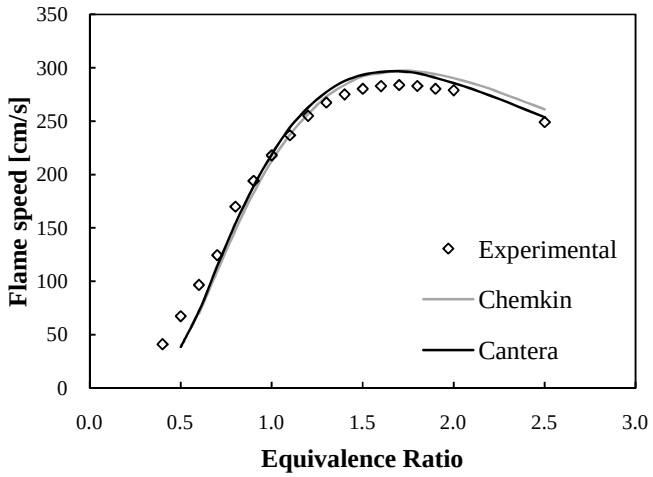

Figure 1 Laminar flame speed comparison between the Cantera and CHEMKIN PRO model for H_2 (GRI3.0, P_i =1 atm, T_i=300K)

Unsteadiness, the presence of complex structures, vortices, enhanced mixing and diffusion, dissipation and fluctuations over broad length and time scales are key characteristics that distinguish turbulent from laminar flow[9]. Turbulence results in greater transport of momentum, species and energy that could not occur with molecular transport alone[10]. Effective thermal conductivity (λ_{eff}), effective viscosity (μ_{eff}) and effective diffusion for species *i* ($D_{i,eff}$), that account for turbulence, are used to describe this enhanced transport introduced by turbulent flow[11]. The λ_{eff} and $D_{i,eff}$ terms replace the corresponding laminar terms in equations (2) and (3). Momentum conservation is not used in unstretched 1D flame solvers, so μ_{eff} is not explicitly used in the conservation equations shown above.

$$\mu_{eff} = \mu_{lam} + \mu_t \quad \text{where} \quad \mu_t = \rho C_\mu \frac{k^2}{\varepsilon} \tag{4}$$

$$\lambda_{eff} = \lambda_{lam} + \lambda_t \quad \text{where} \quad \lambda_t = \frac{C_p \mu_t}{\mathrm{Pr}_t} \tag{5}$$

$$D_{i,eff} = D_{i,m} + D_t \quad \text{where} \quad D_t = \frac{\mu_t}{\rho Sc_t} \tag{6}$$

In these equations, C_μ denotes a constant of 0.09; *k* the turbulent kinetic energy; ε the turbulent dissipation rate; C_p the constant-pressure heat capacity of the mixture; μ_t the turbulent viscosity; Pr_t the turbulent Prandtl number; Sc_t the turbulent Schmidt number. For this version of the solver $\mathrm{Pr_t}$ and $\mathrm{Sc_t}$ are set to constant values of 0.85 and 0.75 respectively.

For combustion to occur, fuel and oxidizer have to mix on the molecular level. In turbulent flames, molecular mixing occurs in micro-mixed turbulent structures known as fine structures[12]. The EDC model is used to describe this mixing and reaction zone in turbulent flow. The model assumes that reactions take place within a perfectly stirred reactor (PSR) with a residence time (τ^*) and length fraction (ξ^*). The length of the PSR is the same as the length scales of the turbulent structures. If the characteristic time for a reaction is greater than τ^* the reaction is quenched. This is implemented within the solver by introducing an effective reaction term, for each species *i*, ($R_{i,eff}$) so that reactions can only occur in the fine structures defined by equation (9). The $R_{i,eff}$ term replaces the corresponding laminar term in equation (2).

$$\tau^* = 0.41\left(\frac{\mu_t}{\rho\varepsilon}\right)^{0.5} \tag{7}$$

$$\xi^* = 2.13\left(\frac{\mu_t \varepsilon}{\rho k^2}\right)^{0.25} \tag{8}$$

$$R_{i,eff} = R_i \cdot \xi^* \tag{9}$$

During turbulent combustion, temperature is represented by temporal mean ($\overline{T}$) and fluctuating (*T'*) values. Due to the highly nonlinear relation between reaction rate constant and temperature, defined by the modified Arrhenius equation, the mean rate constant ($\overline{k}_f$) cannot be calculated using the mean temperature alone, as shown by equation (10). To account for the effect of the fluctuations on each reaction *j*, a correction coefficient (Cc_j) is introduced. Cc_j increases the mean reaction rate such that it is equal to a reaction rate calculated for a kinetic equivalent mean temperature. A Taylor Series expansion of the reaction rate around ($\overline{T}$)[13], equation (11), is used to calculate each value of Cc_j. Mathematically rearranging equation (11) yields equation (12). Although only three terms are shown in equation (12), for Cc_j to reach convergence the Taylor Series expansion requires seven terms. In these equations *A* is pre-exponential factor; β is temperature exponent; E_a is activation energy; $\Re$ is the universal gas constant.

$$\overline{k}_f \neq \mathrm{A} \cdot \overline{T}^{\beta} \exp\left(-\frac{E_a}{\Re \overline{T}}\right) \tag{10}$$

$$\overline{k}_f = k_f(\overline{T}) + \sum_{n=1}^{n=7} \frac{1}{n!} \frac{\delta^n k}{\delta T^n}\bigg|_{\overline{T}} .\mathrm{T}'^n \tag{11}$$

$$\bar{k} = k(\bar{T}) \cdot \left(\begin{array}{l} 1 + \dfrac{\beta\Re + E_a \bar{T}^{-1}}{R} \left(\dfrac{T'}{\bar{T}} \right) + \\ \dfrac{\beta^2\Re^2 - \beta\Re^2 + 2E_a\Re\bar{T}^{-1}(\beta - 1) + E_a{}^2 \bar{T}^{-2}}{2\Re^2} \cdot \left(\dfrac{T'}{\bar{T}} \right)^2 \\ +..... \end{array} \right)$$

$$\bar{k} = k(\bar{T}) \cdot Cc_j \qquad \textbf{(12)}$$

As indicated by equation (12), a steady-state transport equation for temperature variance, T'^2, equation (13), is required for the calculation of Cc_j.

$$\nabla \cdot (\rho u T'^2) = \nabla \cdot \left(\frac{\mu_t}{\sigma_t} \nabla T'^2 \right) + C_g \mu_t (\nabla \bar{T})^2 - C_d \rho \frac{\varepsilon}{k} T'^2 \qquad \textbf{(13)}$$

In this equation, σ_t, C_g and C_d are constants of 0.85, 2.85 and 2.0 respectively[14]. At time of writing, the full ordinary differential equation (ODE), equation (13), had not yet been implemented in Cantera. The following procedure has therefore been adopted. Equation (13) is discretized using the finite difference method (FDM). First and second-order derivatives are approximated using backwards difference (BDS) and central difference (CDS) schemes, respectively. An Excel-based Jacobi iterative solver for T'^2 has been created *external* to Cantera. This solver uses the 1D flow properties calculated by Cantera when enhanced transport and EDC volume fraction are added to the laminar flame speed code. The T'^2 solver requires 800-1,000 iterations to reach a converged profile of $T'^2$and therefore T'. This profile is shown in Figure 2 for Φ = 0.7 and shows a maximum value for T' of ~130 K (T'/T = 0.06.).

Also shown in Figure 2 is the scaled profile of T' found when the diffusion term (1st on right hand side) has been removed from equation (13), and the remainder has been discretized using FDM and BDS only. It is currently possible for this non-diffusive equation to be implemented in Cantera. When diffusion is omitted, the maximum value for T' is ~650 K (T'/T = 0.32), which is unreasonably high. It is however noticed that there is an approximately constant scaling factor (*SF*) between the diffusive and non-diffusive profiles. This trend was found across the range of equivalence ratios studied in this work. For this reason, SF is used to scale the non-diffusive T' profile predicted by the modified Cantera solver to approximate the more accurate profile given by the Excel-based diffusive solver. Work is currently underway to include the solution of equation (13) in the modified Cantera solver.

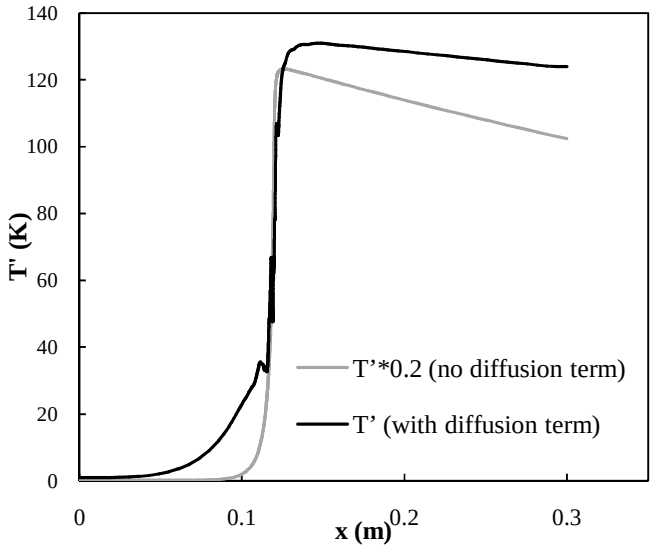

Figure 2 Comparison of the two approaches used to calculate T' for Φ=0.7

Turbulent kinetic energy (k) and turbulent dissipation rate (ε) are used to define the turbulent parameters within the new solver. As the solver will be validated against experimental flame speed data, a method of computing k and ε from readily-available experimental data is needed. For the experiments currently under investigation, values for turbulent intensity, u', and integral length scale, ℓ, are available[15]. The mean Reynolds stresses ($\overline{u_i' u_i'}$) are used to define k. As the solver is 1D, the Reynolds stress in the x direction ($u_x'^2$) is assumed to be equal to the turbulence intensity and zero in the y and z directions, equation (14). The rearranged length scale equation is used to calculate ε, equation (15)[16].

$$k = \frac{1}{2}\overline{u_i' u_i'} = \frac{1}{2}(\overline{u_x'^2} + \overline{u_y'^2} + \overline{u_z'^2})$$
$$\overline{u_x'^2} = \overline{u'^2}; \ \overline{u_y'^2} = \overline{u_z'^2} = 0 \qquad \textbf{(14)}$$
$$\Rightarrow \mathrm{k} = \frac{1}{2}\overline{u'^2}$$

$$\varepsilon = C_\mu^{\frac{3}{4}} \frac{k^{\frac{3}{2}}}{\ell} \qquad \textbf{(15)}$$

Experimental Setup

Experimental turbulent flame speed was previously measured using a spark-ignited cylindrical fan-stirred bomb[15] at Texas A&M University as shown in Figure 3 (a). Four centrally-located, equi-spaced fans produce homogeneous and isotropic turbulence with an average u' of 1.5 m/s and ℓ of 2.7 cm. Flame speeds were measured for H_2 over the range of equivalence ratios $0.5 \leq \Phi \leq 1.0$, at initial temperature and pressure of T_i = 300 K and P_i = 1 atm,

respectively. At these conditions the flames are in the wrinkled and corrugated flamelet regimes, in which the Karlovitz (Ka) number is less than unity. An example of a wrinkled flamelet regime can be seen in Figure 3 (b). Tests were also carried out on methane and methane-hydrogen mixtures, but are beyond the scope of the current work.

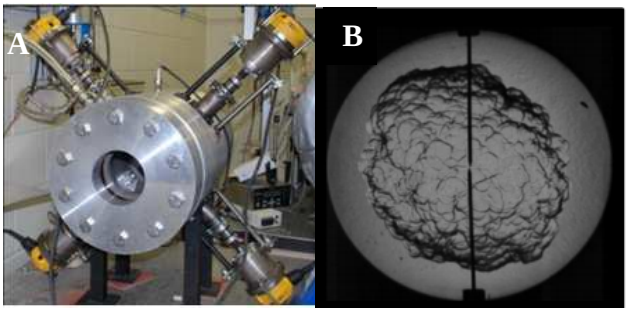

Figure 3(a) Fan-stirred bomb at Texas A&M University; (b) Sample turbulent flame image[15]

Measurements were taken through optical-quality quartz windows located at each end of the vessel. Using high speed Schlieren photography allowed the expanding flame kernel to be tracked to a maximum diameter of 12.7 cm. The flame front area and flame radius were estimated at each frame. A circle with the same equivalent area was then calculated, with the radius equal to the flame radius. To determine S_T the radius's time history was smoothened using a Savitzky-Golay filter and then multiplied by the density ratio (ρ_b / ρ_u). For simplicity and to avoid spark ignition effects the turbulent flame speeds presented here are at a radius equal to integral length scale, 2.7 cm with an effective turbulence intensity of 1.5 m/s.

Validation

A 14-species, 29-reaction hydrogen and syngas mechanism was used for model validation [17]. Multi-component transport equations were used. Adaptive grid parameters were set to obtain grid independent solutions. Equations (13) and (14) were used to define the level of turbulence within the flame. With ℓ = 2.7 cm and u' = 1.5 m/s, k and ε are calculated at 1.125 m^2/s^2 and 7.26 m^2/s^3, respectively. Four cases were modeled, with each successive case introducing additional turbulent effects modelled, as shown in Table 1.

Case	Turbulent effects modelling
Case 1	Laminar only
Case 2	Laminar + Enhanced transport
Case 3	Laminar + Enhanced transport +EDC volume fraction
Case 4	Laminar + Enhanced transport + EDC volume fraction + Enhanced reaction rate

Table 1 Overview of condition for each case

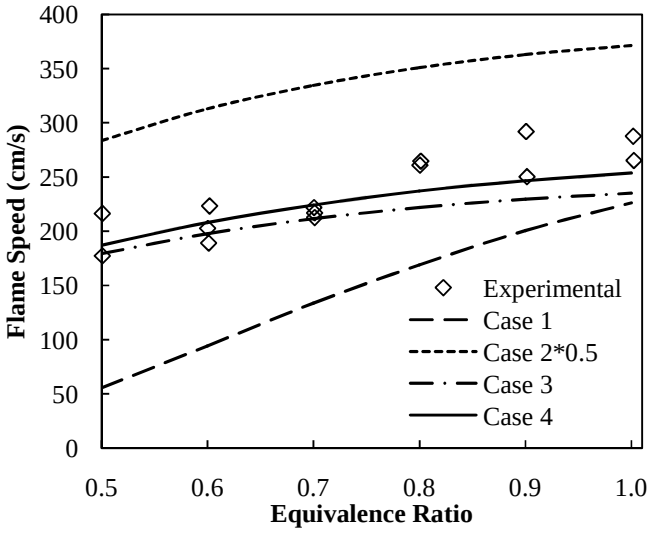

Figure 4 Flame speeds for hydrogen/air mixtures for each case.

Figure 4 shows the flame speed results for hydrogen/air flames for each of the four cases described in Table 1. Case 1 is the base laminar case, in which no turbulent effects are modelled. With the inclusion of enhanced transport, Case 2, the predicated flame speed is three times larger than the experimental values; hence it's scaling by 0.5 for clarity. By limiting the reaction zone with the inclusion of the EDC model, Case 3, the flame speed reduces to values ~90% of the experimental data. The more-lean values calculated for Case 3 are closer to the experimental values by ~5%. For Case 4, with the addition of Cc_j for each reaction, the flame speed increases lightly from the Case 3 values, with a larger increase near stoichiometric conditions. By separately introducing each turbulent effect into the model, their individual impacts can be examined.

In addition to the experimental data an analytical scaling correlation between the laminar and turbulent speed was also calculated, using the third approach outline by Muppala et al [18]. The model predicts turbulent flame speed using the unstretched laminar flame speed along with an exponential Lewis number term, derived from the flame-ball concept of Zel'dovich as shown in equation (16). In this equations Le is the Lewis number and Re_t is the turbulent Reynolds number. The results of the correlation are shown in Figure 5. The correlation matches the data closer to stoichiometric conditions but under estimating flame speeds by a factor of two at $\Phi = 0.5$.

$$\frac{S_T}{S_L} = 1 + \frac{0.46}{e^{(Le-1)}} \mathrm{Re}_t^{0.25} \left(\frac{u'}{S_L} \right)^{0.3} \quad \text{where } Le = \frac{Sc_t}{\mathrm{Pr}_t} \qquad \textbf{(16)}$$

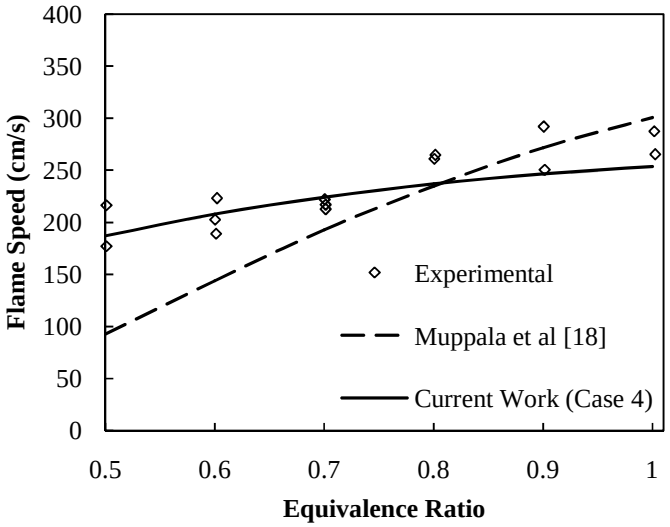

Figure 5 Comparison of experimental, computation and analytical flame speed data for hydrogen/air mixtures

In the case of the hydrogen flames studied, the single greatest turbulent influence on flame speed is seen to be the enhancement of transport due to thermal conduction and species diffusion. These effects lead to 4-5 fold increases in flame speed (Case 2). The reduction in reactivity imposed by the EDC model is seen to be essential in reducing predicted speeds (Case 3). For the flames studied, enhancement of reaction rates is of least importance. A possible explanation for this is the relatively low activation energies present in the hydrogen-air system. This is not the case for hydrocarbon fuels or for NO_x formation reactions. Results indicate that all turbulent effects need to be modelled in order to successfully replicate experimental results.

A flame phenomenon that is not accounted for in this study is flame stretch (κ). For laminar flames stretch is caused by the changing area as the flame propagates outwards, equation (17). In this equation, Ar is the flame area. Unstretched flame length can be obtained using, for example, a linear Markstein relationship from the burnt and stretched flame speed for laminar flames; nonlinear relations are also employed. Turbulent flames exhibit further levels of stretching due to large eddies causing the flame to lose its spherical nature, and small eddies causing flame thickening[19].

$$\kappa = \frac{1}{Ar}\frac{dAr}{dt} \qquad \textbf{(17)}$$

Future Work

Modifications made to the solver have been shown to satisfactorily reproduce experimental data, however further work is required. The method of calculating *T'* currently requires external solution and approximated scaling to a diffusion-free profile. To accurately calculate *T'* the full transport equation must be solved using an ordinary differential equation solver. This will allow for the inclusion of the diffusive term in the solver and will ensure the correct *T'* profile is being used. The presence of flame stretch within the experimental data means it is not completely valid to compare them with the unstretched values predicted by the solver, however for this work it is assumed that flame stretch has only a minor effect when compared to the effect of an incorrect *T'* profile. Finally with these modifications made, the solver will be validated against a range of hydrocarbon fuel blends at various conditions.

Conclusions

A description of the progress made towards a Cantera-based solver to predict turbulent flame speeds has been given. Topics covered include the equations and models added to account for turbulence, the method of calculating temperature fluctuations, details of experimental and computational setups and validation of results. The impacts of the inclusion of models for the turbulent effects are described. Drawbacks with the current procedure are discussed and the future work is identified. The key findings from the paper are:

- It is possible to have a relatively computationally inexpensive 1D turbulent flame solver using Cantera.
- For the flames examined, the incorporation of enhanced transport and an EDC model into a laminar solver will get within ~90% of the experimental measurements.
- A reaction rate correction coefficient is needed to increase the accuracy of the solver to be within reasonable values.

Acknowledgements

The authors are grateful to the Irish Research Council (IRC) and Alstom Power Ltd for co-funding this work with an Enterprise Partnership Scheme Postdoctoral Fellowship Award.

Nomenclature

A	Pre-exponential Factor
C_μ	Constant
Cc_j	Correction Coefficient due to fluctuations
C_p	Constant Pressure Heat capacity
C_q	Constant
C_d	Constant
D	Diffusion Coefficient
E	Total Energy
Ea	Activation Energy
EDC	Eddy Dissipation Concept
J	Diffusional Flux
k	Turbulent Kinetic Energy
k_f	Forward Reaction Rate
Ka	Karlovitz Number
ℓ	Integral Length Scale
Le	Lewis number
P	Pressure
Pr_t	Turbulent Prandtl Number

R_i	Species Source Term
Re_t	Turbulent Reynolds Number
S	Net Heat Production Due to Reactions
Sc_t	Schmidt Number
SF	Scaling Factor
S_L	Laminar Flame Speed
S_T	Turbulent Flame Speed
T	Temperature
T'	Temperature Fluctuations
u	Velocity
Y	Mass Fraction
x	Distance from the burner

Greek Letters

ρ	Density
β	Temperature Exponent
ε	Turbulent Dissipation Rate
λ	Thermal Conductivity
μ	Viscosity
$\Re$	Universal Gas Constant
ξ^*	EDC Length Scale
τ^*	EDC Time Scale
σ_t	Constant
κ	Flame Stretch

Subscripts

b	Burnt
eff	Effective
Lam	Laminar
k	Kinetic Equivalent
i	Species i
t	Turbulent
u	Unburnt

References

[1] United States Energy Information Administration, "International Energy Outlook 2013," 2013.

[2] Reaction Design, "CHEMKIN-PRO," *: San Diego, CA*. Reaction Design, San Diego, CA.

[3] D. Goodwin, N. Nalaya, H. Moffat, and R. Speth, "Cantera: An object-oriented software toolkit for chemical kinetics, thermodynamics, and transport processes." Caltech, Pasadena, 2013.

[4] B. Magnussen, "On the structure of turbulence and a generalized eddy dissipation concept for chemical reaction in turbulent flow," in *19th Aerospace Sciences Meeting*, American Institute of Aeronautics and Astronautics, 1981.

[5] David G. Goodwin and Harry K. Moffat and Raymond L. Speth, "Cantera: An Object-oriented Software Toolkit for Chemical Kinetics, Thermodynamics, and Transport Processes." 2014.

[6] G. Stahl and J. Warnatz, "Numerical investigation of time-dependent properties and extinction of strained methane and propane-air flamelets," *Combust. Flame*, vol. 85, pp. 285–299, 1991.

[7] Z. Q. G.P. Smith, D.M. Golden, M. Frenklach, N.W. Moriarty, B. Eiteneer, M. Goldenberg, C.T. Bowman, R.K. Hanson, S. Song. W.C. Gardiner, V.V Lissianski, "GRI-Mech." [Online]. Available: http://www.me.berkeley.edu/gri_mech/.

[8] E. L. Petersen, N. Donohoe, A. Heufer, and H. J. Curran, "Laminar and Turbulent Flame Speeds for Natural Gas / Hydogen Blends," *Proc. ASME Turbo Expo 2014*, pp. 1–8, 2014.

[9] J. H. Ferziger and M. Peric, *Computational Methods for Fluid Dynamics*. Springer Berlin Heidelberg, 2001.

[10] S. R. Turns, *An introduction to combustion: concepts and applications*, 3rd ed. New York: McGraw-Hill, 1996.

[11] B. E. Launder and D. B. Spalding, *Lectures in mathematical models of turbulence*. Academic Press, 1979.

[12] A. Cuoci, A. Frassoldati, G. Buzzi Ferraris, T. Faravelli, and E. Ranzi, "The ignition, combustion and flame structure of carbon monoxide/hydrogen mixtures. Note 2: Fluid dynamics and kinetic aspects of syngas combustion," *Int. J. Hydrogen Energy*, vol. 32, no. 15, pp. 3486–3500, Oct. 2007.

[13] A. Stagni, A. Cuoci, A. Frassoldati, T. Faravelli, and E. Ranzi, "A fully coupled, parallel approach for the post-processing of {CFD} data through reactor network analysis," *Comput. Chem. Eng.*, vol. 60, no. 0, pp. 197–212, 2014.

[14] L. X. Zhou, L. Qiao, X. L. Chen, and J. Zhang, "A USM turbulence-chemistry model for simulating NO x formation in turbulent combustion q," *Fuel*, vol. 81, no. x, pp. 1703–1709, 2002.

[15] S. Ravi, S. J. Peltier, and E. L. Petersen, "Analysis of the impact of impeller geometry on the turbulent statistics inside a fan-stirred, cylindrical flame speed vessel using PIV," *Exp. Fluids*, vol. 54, 2013.

[16] S. B. Pope, *Turbulent flows*. Cambridge university press, 2000.

[17] A. Kéromnès, W. K. Metcalfe, K. a. Heufer, N. Donohoe, A. K. Das, C. J. Sung, J. Herzler, C. Naumann, P. Griebel, O. Mathieu, M. C. Krejci, E. L. Petersen, W. J. Pitz, and H. J. Curran, "An experimental and detailed chemical kinetic modeling study of hydrogen and syngas mixture oxidation at elevated pressures," *Combust. Flame*, vol. 160, pp. 995–1011, 2013.

[18] S. P. Reddy Muppala, N. K. Aluri, F. Dinkelacker, and A. Leipertz, "Development of an algebraic reaction rate closure for the numerical calculation of turbulent premixed methane, ethylene, and propane/air flames for pressures up to 1.0 MPa," *Combust. Flame*, vol. 140, pp. 257–266, 2005.

[19] I. ANSYS, *ANSYS FLUENT Theory Guide*, vol. 15317, no. November. Canonsburg, 2011.